A Novel Filter for Tracking Real-World Cognitive Stress using Multi-Time-Scale Point Process Observations

Dilranjan S. Wickramasuriya, *Student Member, IEEE* and Rose T. Faghih, *Member, IEEE*

Abstract— Determining the relationship between neurocognitive stress and changes in physiological signals is an important aspect of wearable monitoring. We present a state-space approach for tracking stress from skin conductance and electrocardiography measurements. Individual skin conductance responses (SCRs) are a primary source of information in a skin conductance signal and their rate of occurrence is related to psychological arousal. Likewise, heart rate too varies with emotion. We model SCRs and heartbeats as two different stress-related point processes linked to the same sympathetic nervous system activation. We derive Kalman-like filter equations for tracking stress and use both expectation-maximization and maximum likelihood estimation for parameter recovery. Our preliminary results show that stress is high when a task is unfamiliar, but reduces gradually with familiarity, albeit in the presence of other external stressors. The method demonstrates the feasibility of tracking real-world stress using skin conductance and heart rate measurements. It also serves as a novel state estimation framework for multiple point process observations on different time scales.

I. INTRODUCTION

Stress involves a combination of factors including psychological arousal, a loss of control and unpleasantness [1]. Multiple studies have sought to examine changes in physiological signals during stress (e.g. [2], [3], [4]). Many experiments however, have included tasks such as color-word associations, puzzles and memory problems that only artificially induce stress in participants within laboratory environments. Fewer studies have sought to examine physiological signal changes in response to stress in more realistic environments that resemble actual work spaces with tasks including typical office-like work. Here, we develop a state-space model for tracking stress from skin conductance and heart rate using data collected in such an environment. Heart rate is derived from electrocardiography (EKG) measurements. A skin conductance signal consists of both a slow tonic component and a faster phasic component [5]. Individual skin conductance response (SCR) occurrences make up the phasic component and are used to form a point process. R-peaks are a prominent feature in an EKG signal and co-occur with rhythmic ventricular contractions as the heart pumps blood to the lungs and the rest of the body. These EKG R-peaks form the second point process. The method presented here is an extension of our model in [6] and uses Bayesian filtering for stress state estimation within an iterative Expectation-Maximization (EM) framework.

II. METHODS

A. Data

We use the Smart Reasoning for Well-being at Home and at Work (SWELL) data-set [7]. In it, skin conductance, EKG, computer interactions, video and posture data were recorded from subjects as they engaged in activities typically performed in an office. The tasks included preparing reports and presentations, and responding to e-mails. The experimental trials were divided into three blocks and each subject had to prepare two reports and a Powerpoint presentation (on one of those reports) in every block. In the first block, subjects could take as much time as they liked. In one of the other two blocks, subjects were sent eight e-mails—some of which were irrelevant—and were told to make use of the incoming information and reply as required. In the remaining block, a subject could only take 2/3$^{\text{rds}}$ of the time taken for the very first block. The order of these last two blocks was varied from subject to subject. Here, we label these blocks as the Unfamiliar Task (UT) block (since the subjects were newly introduced to the experimental task), the Repeated Task (RT) block and the Constrained Task (CT) block.

The six report and presentation topics included: stress at work, healthy living, internet privacy, tourist attractions in Perth, the life of Napoleon and details for a road trip across the United States. Two topics were randomly selected each block and subjects were permitted to browse the web in preparing their reports. Each block was preceded by 8 minutes of relaxing music. Here, we provide detailed analysis for one subject (subject 16) over all three blocks.

B. Preprocessing

The skin conductance and EKG data were recorded at 2048 Hz in the SWELL data-set. Many of the skin conductance recordings were heavily noise contaminated. We visually inspected these recordings and selected the subject having the least contamination across all blocks UT, RT and CT. We next manually identified locations where motion artifact corruption was present (usually manifesting as sharp drops) and linearly interpolated over them. We finally lowpass filter the skin conductance at 0.5 Hz similar to [8] and downsample the data to 4 Hz. We also perform peak detection on the EKGs to identify R-peaks.

C. State-space Model

Similar to [6], we assume the subject's stress state X_k follows a random walk with time:

$$X_k = X_{k-1} + \varepsilon_k, \tag{1}$$

where ε_k is zero-mean Gaussian noise having variance σ_ε^2. Skin conductance z_k is a low-bandwidth signal and wearable monitors such as the Empatica E4 record data at a sampling frequency of 4 Hz. We too analyze our data at 4 Hz ($t_s = 0.25$ s). We first decompose the skin conductance into its constituent phasic and tonic parts using cvxEDA [9] and detect SCRs as phasic peaks exceeding a 0.1 threshold. Thereafter, we form a binary point process assigning $M_k = \{1, 0\}$ based on the presence or absence of a peak within each t_s time bin. The occurrence of a peak is a Bernoulli distributed random variable with probability p_k. Using the theory of generalized linear models we relate p_k to X_k using the logit transformation suggested in [10]:

$$\log\left(\frac{p_k}{1 - p_k}\right) = \beta_0 + \beta_1 X_k, \tag{2}$$

where β_0 and β_1 are regression coefficients. Prior work in state estimation from binary data frequently sets $\beta_1 = 1$ and determines β_0 empirically (e.g. [11], [12], [13]). This also helps avoid convergence issues that can occur if both β_0 and β_1 are determined using EM. As in [11], we set $\beta_1 = 1$ letting $p_k = \left[1 + e^{-(\beta_0 + X_k)}\right]^{-1}$ and determine β_0 empirically taking p_0 as the chance probability that a phasic peak occurs at the very outset of the experiment when $X_0 \approx 0$ [6]. $\mathcal{M}^K = \{M_1, M_2, \ldots, M_K\}$ forms our first set of binary observations where each new M_k arrives every t_s.

We next wish to relate heart rate to stress. To do so, we make use of the history-dependent inverse Gaussian (HDIG) probability model [14]. Assume that L consecutive R-peaks occur at times u_l in the interval $(0, T]$ such that $0 < u_1 < u_2 < \ldots < u_L \leq T$, and the lth RR-interval is $w_l = u_l - u_{l-1}$. At time $t > u_l$, the inter-arrival times of the R-peaks can be modeled using an HDIG density function

$$g(t|u_l) = \sqrt{\frac{\theta_{q+1}}{2\pi(t - u_l)^3}} \exp\left\{\frac{-\theta_{q+1}[t - u_l - \hat{\mu}]^2}{2\hat{\mu}^2(t - u_l)}\right\}, \tag{3}$$

where q is the model order, $\hat{\mu} = \theta_0 + \sum_{i=1}^q \theta_i w_{l-i+1}$ and θ_{q+1} is a parameter related to the variance (all the θ_i terms are coefficients to be determined).

Recall that we perform our analysis at 4 Hz. We first divide time into discrete bins of $\Delta = 0.005$ s similar to [14] for HDIG modeling. Therefore, there are $t_s/\Delta = 50$ such bins during each t_s interval, i.e., there are 50 heart rate observation bins for each skin conductance observation M_k (hence forming multi-time-scale point process observations). We index these heart rate bins over $j = 1, 2, \ldots, J$, where $J = 50$. Thereafter, each bin is assigned $N_{k,j} = 1$ or $N_{k,j} = 0$ based on whether or not an R-peak occurs within it. The joint probability over these J observations is [15],

$$P(N_{k,1}, N_{k,2}, \ldots, N_{k,J}) = e^{\sum_{j=1}^J \log(\lambda_{k,j}\Delta)n_{k,j} - \lambda_{k,j}\Delta} \tag{4}$$

where $\lambda_{k,j}$ is the conditional intensity function (CIF)

$$\lambda_{k,j} \triangleq \frac{g(t_{k,j}|u_{k,j})}{1 - \int_{u_{k,j}}^{t_{k,j}} g(z|u_{k,j})dz}, \tag{5}$$

with $u_{k,j}$ being the time that the last R-peak occurred prior to $t_{k,j}$. The joint density function accounts for the

R-peak history at each point via $\lambda_{k,j}$ and does not require independence over $N_{k,j}$. In order to incorporate the stress state X_k into the HDIG model, we modify $\hat{\mu}$ and define $\mu = \theta_0 + \sum_{i=1}^q \theta_i w_{l-i+1} + \eta X_k$ as the new stress-dependent mean; here η is a parameter to be determined. Accordingly, we expect the HDIG density function to shift either to the left or to the right as stress levels change. $\mathcal{N}^K = \{N_{1,1}, \ldots, N_{1,J}, N_{2,1}, \ldots, N_{2,J}, \ldots, N_{K,1}, \ldots, N_{K,J}\}$ forms the second set of binary observations.

D. Estimation

1) Expectation-Step: Given $\mathcal{M}^K$ and $\mathcal{N}^K$, we wish to determine $X_k \ \forall k$. The present work is a novel filter for estimating X_k combining skin conductance and heart rate at two different time scales. Letting $\mathcal{Y}^k = \{\mathcal{M}^k, \mathcal{N}^k\}$ denote the observations up to the kth time instance, we make a Gaussian approximation to the posterior density $f_{X_k|\mathcal{Y}^k}(x_k|y^k)$ similar to [16] to derive the following Kalman-like forward filter equations for $k = 2 : K$:

Predict:
$$x_{k|k-1} = x_{k-1|k-1} \tag{6}$$
$$\sigma_{k|k-1}^2 = \sigma_{k-1|k-1}^2 + \sigma_\varepsilon^2 \tag{7}$$

Update:
$$x_{k|k} = x_{k|k-1} + \sigma_{k|k-1}^2 \left[(m_k - p_{k|k})\right.$$
$$\left. + \sum_{j=1}^J \frac{1}{\lambda_{k,j|k}} \frac{\partial \lambda_{k,j|k}}{\partial x_k}(n_{k,j} - \lambda_{k,j|k}\Delta)\right] \tag{8}$$

$$\sigma_{k|k}^2 = \left\{\frac{1}{\sigma_{k|k-1}^2} + p_{k|k}(1 - p_{k|k})\right.$$
$$- \sum_{j=1}^J \left[\frac{1}{\lambda_{k,j|k}} \frac{\partial^2 \lambda_{k,j|k}}{\partial x_k^2}(n_{k,j} - \lambda_{k,j|k}\Delta)\right.$$
$$\left.\left. - \frac{n_{k,j}}{\lambda_{k,j|k}^2}\left(\frac{\partial \lambda_{k,j|k}}{\partial x_k}\right)^2\right]\right\}^{-1} \tag{9}$$

We solve (8) using Newton's method as $x_{k|k}$ appears on both sides of the equality sign. The smoothed estimates are [11],

$$A_k \triangleq \frac{\sigma_{k|k}^2}{\sigma_{k+1|k}^2} \tag{10}$$

$$x_{k|K} = x_{k|k} + A_k(x_{k+1|K} - x_{k+1|k}) \tag{11}$$

$$\sigma_{k|K}^2 = \sigma_{k|k}^2 + A_k^2(\sigma_{k+1|K}^2 - \sigma_{k+1|k}^2). \tag{12}$$

2) Maximization-Step: We determine the noise variance of the random walk σ_ε^2 using EM. Defining the following,

$$U_k \triangleq x_{k|K}^2 + \sigma_{k|K}^2 \tag{13}$$
$$U_{k,k+1} \triangleq x_{k|K}x_{k+1|K} + A_k\sigma_{k+1|K}^2 \tag{14}$$

the variance update for the $(n+1)^{\text{th}}$ iteration is given by,

$$\sigma_\varepsilon^{2(n+1)} = \frac{1}{K}\left[\sum_{k=2}^K U_k - 2\sum_{k=1}^{K-1} U_{k,k+1} + \sum_{k=1}^{K-1} U_k\right]. \tag{15}$$

Here, we have set $X_0 = X_1$ instead of treating it as a separate parameter similar to one of the options provided in [11], [12]. This allows for some bias at the beginning.
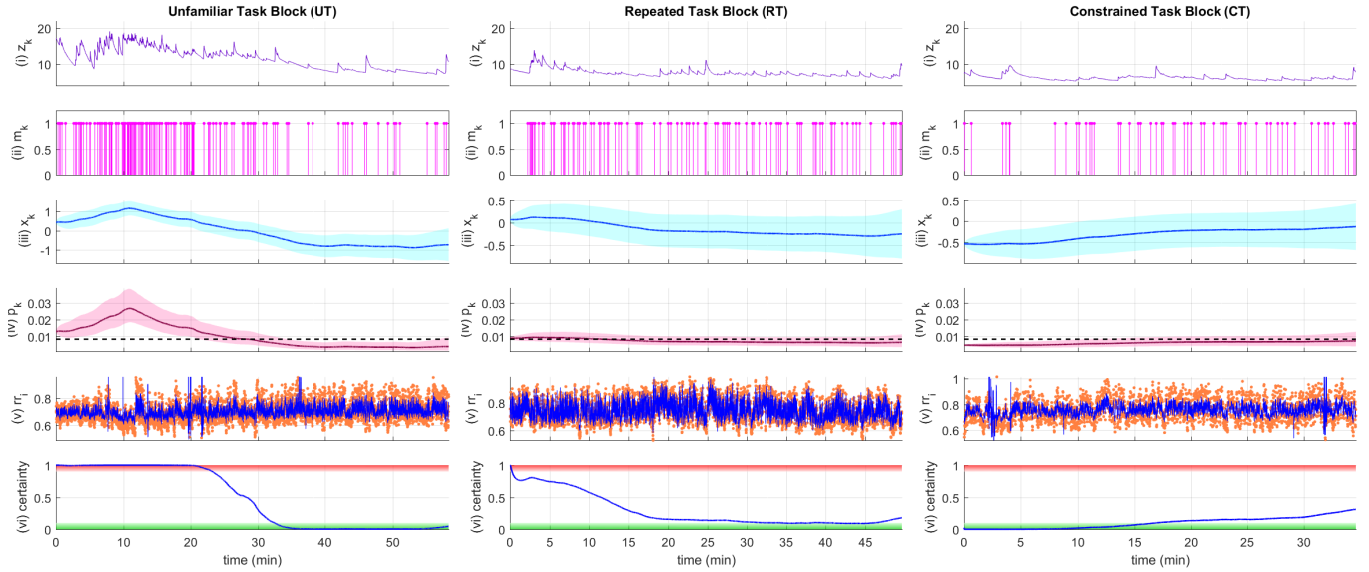
Fig. 1: **Stress state estimation.** In each sub-figure, the sub-panels in turn depict, (i) the skin conductance signal; (ii) the phasic SCR peak occurrences; (iii) the stress estimate $x_{k|K}$ and its confidence limits; (iv) the probability of a phasic SCR peak occurrence $p_{k|K}$ and its confidence limits (the black dashed line indicates the baseline probability p_0); (v) RR-intervals (orange dots) and HDIG model fits (blue line); (vi) stress certainty level with the upper and lower portions highlighting the region above 90% (red) and below 10% (green) respectively.

Determining η requires us to maximize the following expected log-likelihood term:

$$Q = \sum_{k=1}^{K} \sum_{j=1}^{J} \mathbb{E}\big[\log(\lambda_{k,j}\Delta)n_{k,j} - \lambda_{k,j}\Delta\big]. \quad (16)$$

Maximizing Q with respect to η is prohibitively time consuming in MATLAB. Therefore, we perform a Taylor series expansion around each $x_{k|K}$ and try a fixed set of η values and choose the best one that maximizes Q. As heart rate generally speeds up with stress causing RR-intervals to decrease, we searched *negative* values for η ranging from $(-1) \times 10^{-5}$ to $(-1) \times 10^{-4}$ in increments of 10^{-5}.

3) Maximum Likelihood Estimation: The values for $\Theta = \{\theta_0, \theta_1, \ldots, \theta_{q+1}\}$ were likewise not determined using EM due to time consumption. Instead the best Θ was calculated via maximum likelihood considering the complete RR-interval time series [14]. Model fits to the RR-intervals are evaluated using a Kolmogorov-Smirnov (KS) plot [14]. The KS distance in a KS plot provides a measure of how well the model fits to the observed data. Barbieri *et al.* [14] selected $q = 2, 4$ for their experimental data based on Akaike's information criteria and KS plots. Following their approach, we explored orders $q = 1, 2, 3, 4$ and selected the $q = 3$ as the one with the smallest KS distance across all three trial blocks. Higher orders for q could also be investigated.

E. Certainty Level of Stress

Similar to [11], a certainty level of stress can be calculated using the probability density function of p_k

$$f(p_k) = \frac{1}{\sqrt{2\pi\sigma_{k|K}^2}\,p_k(1-p_k)}$$

$$\cdot \exp\left\{\frac{-1}{2\sigma_{k|K}^2}\left[-x_{k|K} + \log\frac{p_k}{(1-p_k)e^{\beta_0}}\right]\right\}. \quad (17)$$

The stress certainty level is the probability that $p_k > p_0$, i.e., a measure of how certain we are that phasic SCR peaks are occurring more than just by chance. This could equivalently be calculated based on the state estimates for X_k.

III. RESULTS

Stress estimates for the three experimental blocks and corresponding KS plots are shown in Figs. 1 and 2 respectively. Stress levels as measured by the certainty level are highest at the start of the experiment in block UT and gradually decrease. Here, stress certainty exceeds 90% for about the first 20 minutes. In block RT, stress certainty does not exceed 90% even once, although it is highest at the start of the block. Stress remains lowest during block CT and a gradual increase can be seen as the experiment progresses. This may be expected as the subject had to complete the writing tasks within the shortened time limit. The raw skin conductance *level* also contains information regarding arousal [17], although we have not taken it into
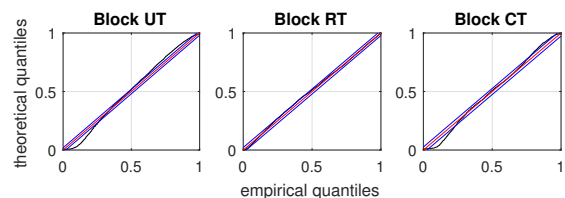

Fig. 2: **KS plots**. The plots indicate the goodness of fit of the CIF to the RR-intervals.

account here. z_k decreases from block UT, to RT, to CT indicating a decline in arousal as the experiment proceeds.

The KS plots do not fall entirely within the 95% confidence limits although there is close agreement. In general, the better the CIF for modeling heart rate, the closer will be the plot to the 45° diagonal. Fig. 3 appears to show some irregularity in the subject's EKG. The unusually large RR-intervals may have caused errors in the HDIG model fits.
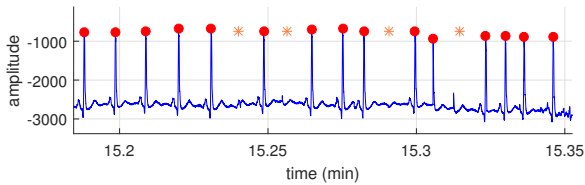

Fig. 3: **A section of the subject's EKG**. The red dots depict R-peaks and the orange stars depict locations of possible EKG irregularities.

IV. DISCUSSION

The experiment in [7] was originally designed to examine psychological stress in the presence of external interruptions and time restriction pressures. While interruptions and time constraints do cause anxiety, our analysis seems to point out that *unfamiliarity* or how new a task is to someone seems to have caused the most stress to subject 16. It may be the case that unfamiliarity with a task dominates the anxiety caused by both time constraints and unnecessary interruptions.

Stress is a subjective experience. Participants in the SWELL data-set gave single-number estimates of how they felt with regard to different aspects (e.g. arousal, valence, dominance) during each task block. Variability often exists in subjective ratings. The features we track are related to how much a person's sympathetic nervous system is activated. Our method therefore provides an unsupervised approach for tracking stress continuously in the absence of labels.

V. CONCLUSIONS

We present a state-space model for tracking stress using skin conductance and EKG measurements. The model was evaluated on a single subject in the SWELL data-set across three experimental conditions. Our preliminary results point to the fact that unfamiliarity with a task appears to be the primary cause of stress in this experiment. Future work would involve including the effect of skin conductance level into the model and developing an adaptive filter for motion artifact removal. We also plan to perform further validation with experimental data. Here, we used a peak detection method here for locating SCRs. A further improvement would be to incorporate the sparse deconvolution scheme in [18], [19], [20], [21] to determine SCR timing and amplitude more precisely.

REFERENCES

[1] G. Fink, "Chapter 1 - stress, definitions, mechanisms, and effects outlined: Lessons from anxiety," in *Stress: Concepts, Cognition, Emotion, and Behavior*, pp. 3 – 11, San Diego: Academic Press, 1st ed., 2016.

[2] A. Sano and R. W. Picard, "Stress recognition using wearable sensors and mobile phones," in *Proc. Humaine Assoc. Conf. Affective Comput. and Intell. Interaction*, pp. 671–676, 2013.

[3] D. C. M. B. P. Birjandtalab, Javad and M. Nourani, "A non-EEG biosignals dataset for assessment and visualization of neurological status," in *Proc. IEEE Int. Workshop Signal Process. Syst.*, pp. 110–114, 2016.

[4] J. Wijsman, B. Grundlehner, H. Liu, H. Hermens, and J. Penders, "Towards mental stress detection using wearable physiological sensors," in *Proc. Annu. Int. Conf. IEEE Eng. in Medicine and Biology Society*, pp. 1798–1801, 2011.

[5] M. Benedek and C. Kaernbach, "Decomposition of skin conductance data by means of nonnegative deconvolution," *Psychophysiology*, vol. 47, no. 4, pp. 647–658, 2010.

[6] D. S. Wickramasuriya, C. Qi, and R. T. Faghih, "A state-space approach for detecting stress from electrodermal activity," in *Proc. 40th Annu. Int. Conf. IEEE Eng. Medicine and Biology Society*, pp. 3562–3567, 2018.

[7] S. Koldijk, M. Sappelli, S. Verberne, M. A. Neerincx, and W. Kraaij, "The SWELL knowledge work dataset for stress and user modeling research," in *Proc. Int. Conf. Multimodal Interaction*, pp. 291–298, ACM, 2014.

[8] S. Doberenz, W. T. Roth, E. Wollburg, N. I. Maslowski, and S. Kim, "Methodological considerations in ambulatory skin conductance monitoring," *Int. J. Psychophysiology*, vol. 80, no. 2, pp. 87–95, 2011.

[9] A. Greco, G. Valenza, A. Lanata, E. P. Scilingo, and L. Citi, "cvxEDA: A convex optimization approach to electrodermal activity processing," *IEEE Trans. Biomed. Eng.*, vol. 63, no. 4, pp. 797–804, 2016.

[10] P. McCullagh and J. A. Nelder, *Generalized Linear Models*, vol. 37. CRC press, 1989.

[11] A. C. Smith, L. M. Frank, S. Wirth, M. Yanike, D. Hu, Y. Kubota, A. M. Graybiel, W. A. Suzuki, and E. N. Brown, "Dynamic analysis of learning in behavioral experiments," *J. Neuroscience*, vol. 24, no. 2, pp. 447–461, 2004.

[12] M. J. Prerau, A. C. Smith, U. T. Eden, Y. Kubota, M. Yanike, W. Suzuki, A. M. Graybiel, and E. N. Brown, "Characterizing learning by simultaneous analysis of continuous and binary measures of performance," *J. Neurophysiology*, vol. 102, no. 5, pp. 3060–3072, 2009.

[13] X. Deng, R. T. Faghih, R. Barbieri, A. C. Paulk, W. F. Asaad, E. N. Brown, D. D. Dougherty, A. S. Widge, E. N. Eskandar, and U. T. Eden, "Estimating a dynamic state to relate neural spiking activity to behavioral signals during cognitive tasks," in *Proc. 37th Annu. Int. Conf. IEEE Eng. Medicine and Biology Society*, pp. 7808–7813, 2015.

[14] R. Barbieri, E. C. Matten, A. A. Alabi, and E. N. Brown, "A point-process model of human heartbeat intervals: new definitions of heart rate and heart rate variability," *American J. Physiology-Heart and Circulatory Physiology*, vol. 288, no. 1, pp. H424–H435, 2005.

[15] U. T. Eden, L. Srinivasan, and S. V. Sarma, "Nueral signal processing tutorial II: Point process model estimation and goodness-of-fit analysis," in *Neural Signal Processing: Quantitative Analysis of Neural Activity* (P. Mitra, ed.), ch. 9, pp. 79–87, Washington DC: Society for Neuroscience, 2008.

[16] T. P. Coleman, M. Yanike, W. A. Suzuki, and E. N. Brown, "A mixed-filter algorithm for dynamically tracking learning from multiple behavioral and neurophysiological measures," *The Dynamic Brain: An Exploration of Neuronal Variability and its Functional Significance*, pp. 3–28, 2011.

[17] W. Boucsein, *Electrodermal Activity*. New York, NY: Springer Science & Business Media, 2nd ed., 2012.

[18] M. R. Amin and R. T. Faghih, "Inferring autonomic nervous system stimulation from hand and foot skin conductance measurements," in *Proc. 52nd Asilomar Conf. Signals, Systems and Computers*, Oct 2018.

[19] M. R. Amin and R. T. Faghih, "Sparse deconvolution of electrodermal activity via continuous-time system identification," *IEEE Trans. Biomed. Eng.*, 2019.

[20] R. T. Faghih, P. A. Stokes, M.-F. Marin, R. G. Zsido, S. Zorowitz, B. L. Rosenbaum, H. Song, M. R. Milad, D. D. Dougherty, E. N. Eskandar, and R. Barbieri, "Characterization of fear conditioning and fear extinction by analysis of electrodermal activity," in *37th Annu. Int. Conf. IEEE Eng. Medicine and Biology Society*, pp. 7814–7818, 2015.

[21] R. T. Faghih, "From physiological signals to pulsatile dynamics: A sparse system identification approach," in *Dynamic Neuroscience*, pp. 239–265, Springer, 2018.